CIVIL ENGINEERING JOURNAL

Article no. 37

THE CIVIL ENGINEERING JOURNAL 3-2022

STUDY ON TIME-DEPENDENT OF BEARING CAPACITY OF OFFSHORE LARGE-DIAMETER MONOPILES

Suchun Yang[1 2], Qiang Chen [2], Shean Bie [1] and Fubo He [2]

1. *Tianjin University, School of Civil Engineering, Tianjin; China; e-mail：18560609732@qq.com*
2. *Tianjin Port and Channel Engineering Co., Ltd., Tianjin, China*

ABSTRACT

To improve the accuracy of predicting the bearing capacity of offshore large-diameter monopiles, the initial high strain detection and repeated high strain detection with an interval of 10-84 days were carried out on 6 large-diameter monopiles with a diameter of 7.2m-7.4m in the offshore wind field dominated by clay soil layer. The results show that the time-dependent increment of tip resistance, side resistance and the total resistance of large-diameter monopiles in the same offshore wind farm has great discreteness, and the axial force increment of monopiles has a consistent change trend. This paper puts forward the prediction interval of 95% guarantee rate of bearing capacity increment of the offshore large-diameter monopiles based on depth, which provides a basis for the design of large-diameter monopiles.

KEYWORDS

Offshore, Large diameter, Monopiles, Side resistance, Time-dependent

INTRODUCTION

As the most common foundation type of offshore wind turbine [1], large-diameter monopiles are widely used in sea areas where the sea depth does not exceed 35m. Large-diameter monopiles can only be driven by a hammer with high strike energy. The process of driving monopiles by hammer with high strike energy will weaken the soil around the pile. The high strain detection after the monopiles reach the design elevation can only obtain a small bearing capacity, and there is often no effective bearing capacity near the pile head. Offshore strata often have thick weak layers, and offshore monopiles need to be embedded at great depth in the mud to meet the requirements of bearing capacity. They often cross several soil layers, and the calculation of bearing capacity is cumbersome. After the rest period, the high strain detection of monopiles requires the ship to be stationed again, which is difficult and costly. The mechanical properties of offshore monopiles from driving to using are different from those of onshore small-size piles, and their time effect also shows great differences [3]. Existing research results [4-8] are difficult to meet the needs of engineering practice. In particular, the design basis for monopile bearing capacity in API and DNV specifications[9, 10] are derived from the test data of small-diameter pile foundation [11, 12], and the size effect significantly affects the bearing capacity of pile foundation [13], which is not well applicable to large-diameter monopiles.

TEST OVERVIEW

The test site is the No. 4 offshore wind farm in the south of the Shandong Peninsula, located in the sea area in the south of Haiyang City, Shandong Province, with an offshore distance of about 30km. The seabed terrain changes gently with a water depth of 29-31m. The surface layer of foundation soil in the site area is mainly muddy silty clay, silty clay and silty soil. The survey conditions and static cone penetration parameters of the test pile base are shown in Table 1.

High strain detections were carried out immediately after 6 large-diameter monopiles were hammered and sunk, and high strain detections were carried out after a certain rest period, as shown in Figure 1. Among them, 4 large-diameter monopiles obtained a relatively complete pile shaft force distribution curve, and the pile shaft parameters are shown in Table 2.

Tab. 1: Geological parameters of the test site

Monopile 1			Monopile 2			Monopile 3			Monopile 4		
Soil layer	Bottom height/m	Side friction /kPa	Soil layer	Bottom height/m	Side friction /kPa	Soil layer	Bottom height/m	Side friction /kPa	Soil layer	Bottom height/m	Side friction /kPa
Mud top	-29		Mud top	-30		Mud top	-30		Mud top	-31	
Muddy silty clay	-32	9	Muddy silty clay	-35	9	Muddy silty clay	-37	9	Muddy silty clay	-40	9
Silty clay	-33	21	Silt	-38	50	Silty clay	-39	21	Silt with sand	-42	53
Silt with sand	-36	53	Silty clay	-48	21	Sand with silt	-40	93	Sand with silt	-47	93
Silty clay	-45	21	Sand with silt	-50	93	Silt with sand	-41	53	Silty clay	-51	21
Silt with sand	-46	53	Silt with sand	-55	53	Silty clay	-50	21	Silt with sand	-53	53
Silty clay	-46	37	Sand with silt	-57	171	Sand with silt	-51	93	Silty clay	-60	37
Sand with silt	-49	93	Silt with sand	-58	53	Silty clay	-52	37	Silt with sand	-65	124
Silty clay	-56	37	Sand with silt	-62	171	Medium sand	-57	201	Silty clay	-69	52
Sand with silt	-57	171	Silty clay	-63	52	Silt with sand	-58	124	Silt with sand	-75	124
Silty clay	-58	52	Silt with sand	-67	124	Silty fine sand	-61	222	Silty clay with silt	-80	50
Medium sand	-59	201	Silty fine sand	-71	222	Silt with sand	-62	124	Pile tip	3.08 MPa	
Silty clay	-61	52	Pile tip	20.89 MPa		Silty clay with silt	-66	50			
Silt with sand	-64	124				Silt with sand	-67	125			
Silty fine sand	-65	222				Silty clay with silt	-73	50			
Silty clay	-67	52				Silt with sand	-75	125			
Silty fine sand	-68	222				Silty fine sand	-78	446			

Silty clay with silt	-72	50			Pile tip	31.47MPa		
Pile tip	3 MPa							

Fig. 1 – High strain detection of large-diameter monopile

Tab. 2: Monopile parameters

Monopile No.	Length/m	Mud elevation/m	Pile tip elevation/m	Penetration depth/m	Pile diameter /m	Pile tip thickness /mm	Pile tip area / m^2
1	84	-28.65	-72	43.35	7.2	70	1.57
2	81	-29.8	-69	39.2	7.2	70	1.57
3	88	-30.5	-76	45.5	7.4	72	1.66
4	88	-30.8	-76	45.2	7.2	70	1.57
5	92	-29.9	-80	50.1	7.4	70	1.61
6	86.5	-30.5	-74.5	44	7.2	70	1.57

TEST RESULTS AND ANALYSIS

After the initial driving high strain detections of No. 1-6 piles were completed, the repeated driving high strain detections were carried out at an interval of 10d-84d. The change of monopiles bearing capacity is shown in Table 3. The results of the literature [14] show that most of the bearing capacity of offshore monopiles can be recovered within 24h. The bearing capacity data in Table 3 shows that when the rest period exceeds 10d, the increase of pile tip resistance, pile side resistance and total bearing capacity does not increase with time, which is consistent with the research results in the literature [14].

Tab. 3: Bearing capacity of monopiles

Pile No.	Stage	Pile side resistance /kN	Pile tip resistance /kN	Total resistance /kN	Side resistance increment /kN	Tip resistance increment /kN	Total resistance increment /kN	Side resistance growth rate /%	Tip resistance growth rate /%	Total resistance growth rate /%	Rest period /d
1	Initial	7685	10064	17749	22807	6006	28813	297	60	162	34
	Repeated	30492	16070	46562							
2	Initial	19514	10014	29528	12780	6351	19131	65	63	65	31
	Repeated	32294	16365	48659							
3	Initial	23047	7898	30945	17073	5406	22479	74	68	73	10
	Repeated	40120	13304	53424							
4	Initial	18171	3926	22097	25821	2040	27861	142	52	126	18
	Repeated	43992	5966	49958							
5	Initial	19060	6527	25587	38147	910	39057	200	14	153	54
	Repeated	57207	7437	64644							
6	Initial	22243	6328	28571	29182	923	30105	131	15	105	84
	Repeated	51425	7251	58676							

Time-dependent tip resistance

When the pile tip is in the silty fine sand layer, the growth rate of pile tip resistance is relatively consistent. Table 3 shows that the pile tip resistance increases by 63%-68% after the 10d-31d rest period.

Similarly, the growth rate of pile tip resistance also shows a similar law when the pile tip is in silty clay mixed with silty, and the pile tip resistance increases by 52%-60% after the 18-34 day rest period.

From the perspective of soil bearing capacity, silty clay, silty clay mixed with silt, and silty soil mixed with silt are enhanced in turn. The soil layer at the pile tip of the No. 6 pile is silty soil mixed with silt, but the pile tip resistance is only increased by 15% after the 84-day rest period, which is far lower than the 52% increase in the 18-day rest period of No. 4 pile. According to the bearing capacity of the soil, the restoring capacity of soil can not be well judged.

Time-dependent side resistance

It can be seen from Table 1 that more than 75% of the stratum where the test pile is located is the clay soil layer, the side resistance of the No. 3 pile increases by 74% in 10d, and the total friction of No. 1 pile increases by 297% in 34d. This difference in increase is not caused by time accumulation, but due to the weakening of soil around the pile caused by heavy blows, or even the occurrence of liquefaction. Whether the weakening range of soil around the pile is concentrated at the pile tip, there is no definite answer for large diameter monopiles. The recovery value of the pile side resistance can quantify the degree of weakening of the soil around the pile. The recovery value of the side resistance of each section is shown in Table 4.

Tab. 4: Recovery value of side resistance of each section of piles

Pile shaft section	No. 1 pile/kN	No. 2 pile/kN	No. 3 pile/kN	No. 4 pile/kN
1/4	7978	3005	3834	3653
2/4	7667	2135	2713	2363
3/4	4994	2819	4608	4612
4/4	2167	4820	5919	7550

It can be seen from Table 4 that the peak value of side resistance recovery is uncertain in a certain section, indicating that the impact energy during pile sinking can be dispersed in the soil around the whole pile.

Time-dependent total resistance

It can be seen from Table 3 that the increase of total resistance after 10d-84d rest period is 65%-162%, and the soil layer in the same wind farm is relatively uniform, but the increase of total resistance of large-diameter monopiles fluctuates greatly, which is due to the large difference in residual bearing capacity of each pile position after initial driving. The axial force of No. 1-4 piles during initial driving and repeated driving is shown in Figure 2. According to Table 3, the total resistance of No. 1 pile after initial driving is 17749kN, while the total resistance of No. 3 pile is 30945kN, with a large difference. The number of hammers and the hammering energy used in the process of pile sinking are mainly determined by factors such as the nature of the stratum, the self-weight of the pile body, hammering equipment, etc. even if the same wind farm and different pile positions will have the phenomenon of pile sliding and hammer refusal, which also makes it difficult to quantify the weakening of the soil around the pile.

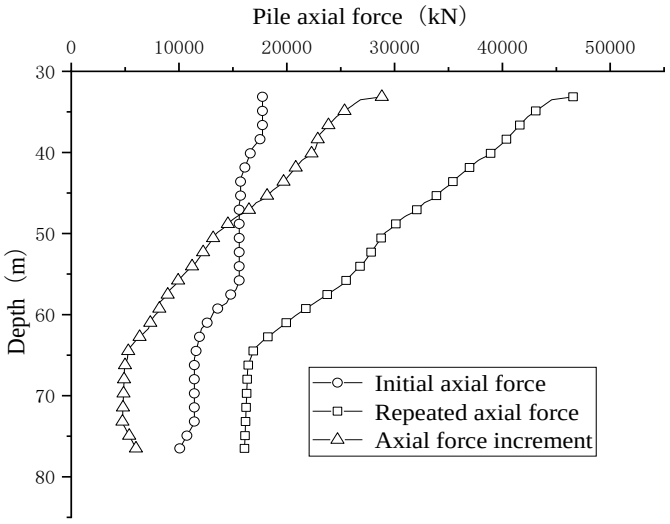

（1）No. 1 pile

Fig. 2 – Initial driving and repeated driving of axial force

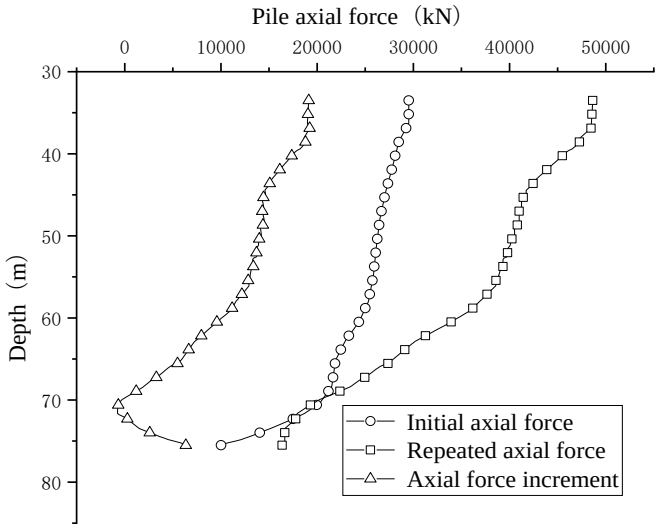

（2）No. 2 pile

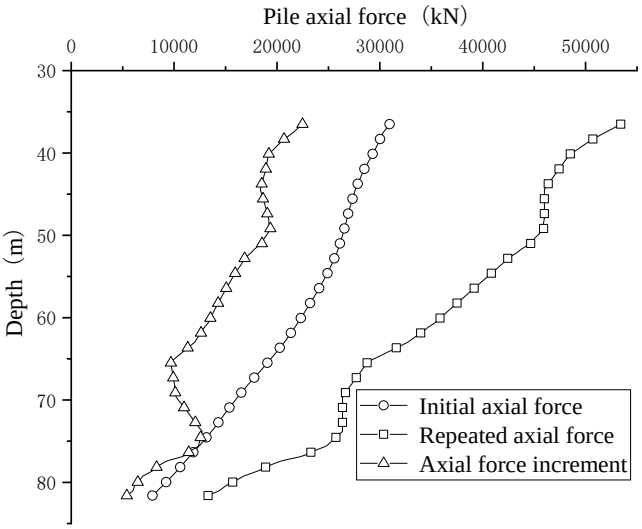

（3）No. 3 pile

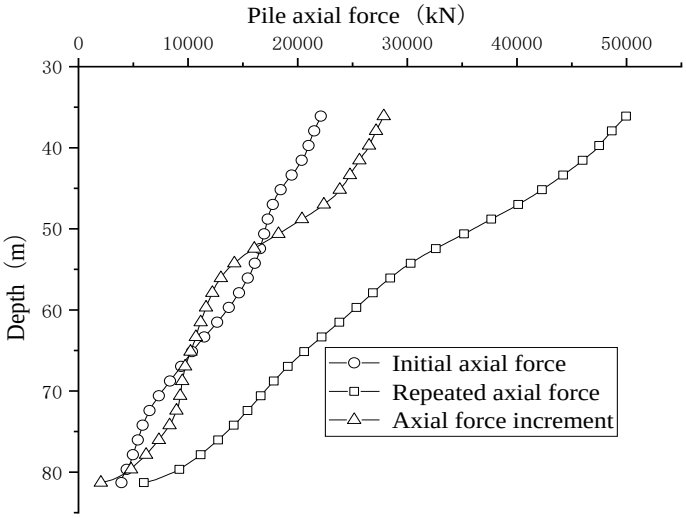

（4）No. 4 pile

Fig. 2 – Initial driving and repeated driving of axial force

Comparison of bearing capacity

The bearing capacity of large-diameter monopiles can be calculated by Equation (1) according to the side resistance per unit area and pile tip resistance per unit area in Table 1.

$$Q_u = Q_{su} + Q_{pu} = u_i \sum l_i q_{sui} + A_p q_{pu} \quad (1)$$

Where Q_u is the bearing capacity of monopile, Q_{su} is the total side resistance, Q_{pu} is the total tip resistance, u_i is the circumference of pile in layer i, l_i is the thickness of layer i, q_{sui} is unit side resistance of layer i, q_{pu} is unit tip resistance of layer i, and A_p is pile tip area.

The calculation results of No. 1-4 piles are compared with the measured values as shown in Figure 3.

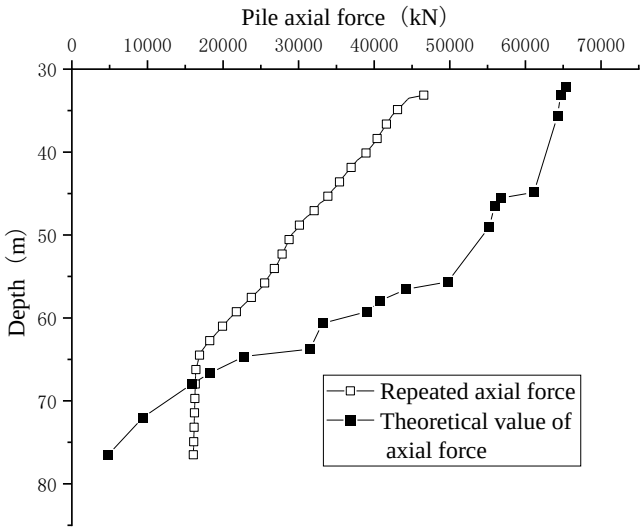

(1) No. 1 pile

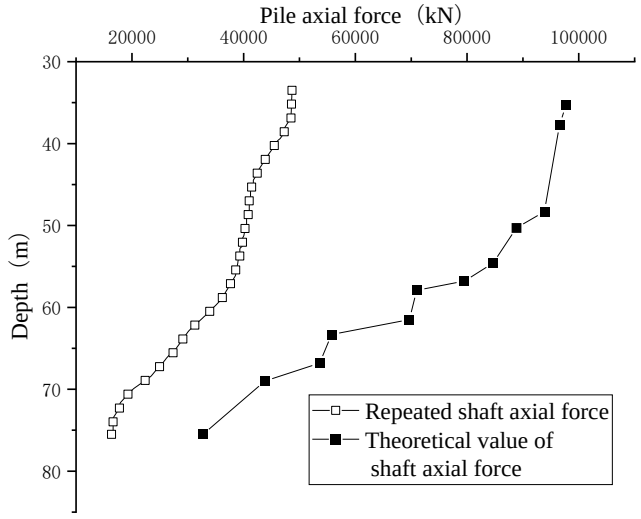

(2) No. 2 pile

Fig. 3 – Repeated driving and theoretical value of axial force

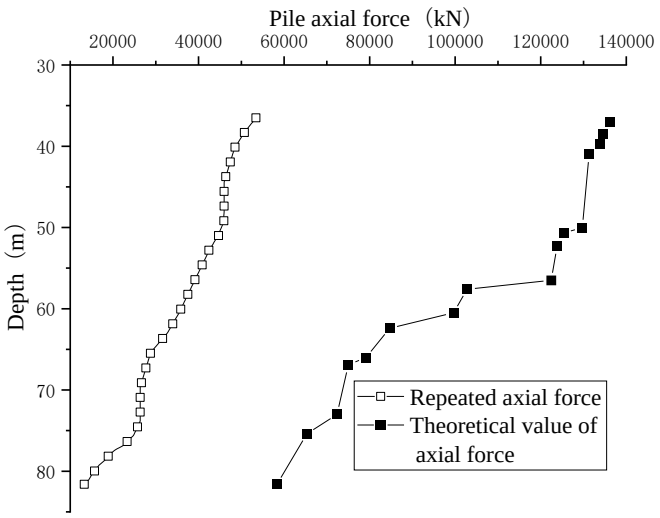

(3) No. 3 pile

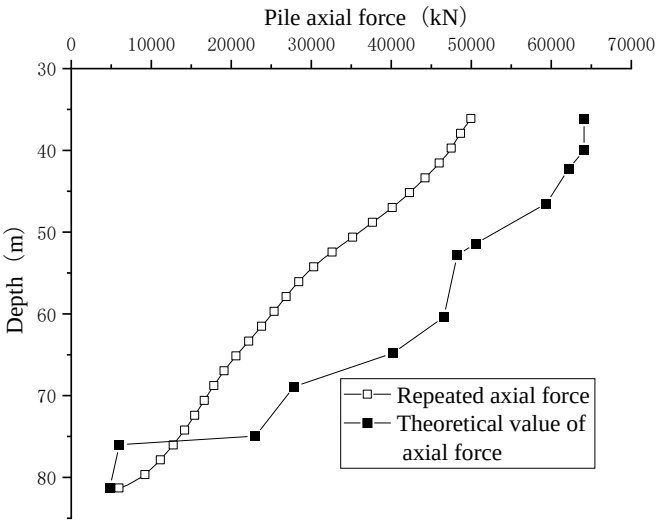

(4) No. 4 pile

Fig. 3 – Repeated driving and theoretical value of axial force

According to literature [15], the axial force of the pile can be recovered by more than 90% after being driven for 6d. The rest period of this test is far beyond 6d, and the soil shear test parameters obtained from the indoor test cannot accurately calculate the axial force. It can be seen from Figure 3 that there is a huge difference between the measured value and the calculated value. Therefore, a more effective way is needed to predict the axial force.

Depth fitting method

Since the time-dependent increase of side resistance and tip resistance is relatively discrete, it cannot be calculated based on the stressed area and the strength per unit area. However, the change of the axial force increment shows a good linear relationship with the depth, as shown in Figure 4, and the axial force increment has a relatively consistent change trend, which can be predicted according to formula (2), with a good assurance rate.

$$\Delta Q = -415\mathrm{h} + 36315 \pm l \tag{2}$$

Where, ΔQ is the axial force increment (kN), h is the depth (m), and l is the upper and lower limit adjustment coefficient of 95% prediction band (5460kN in this example).

The existing large-diameter monopiles have high strain detection after the pile penetration process. The pile shaft axial force lower limit value with a 95% assurance rate can be superimposed on the initial driving bearing capacity to provide a good basis for the design.

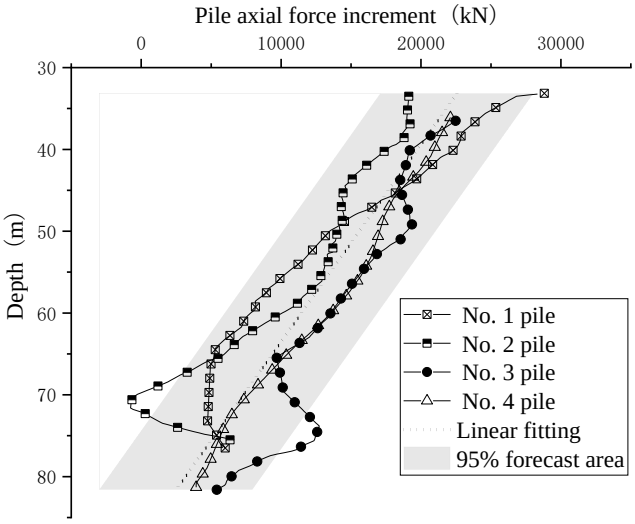

Fig. 4 –Variation trend of axial force increment

CONCLUSION

Due to the disturbance of the soil around the pile during the driving process, the bearing capacity of the driven pile is difficult to be calculated by the existing formula. Based on the initial high strain detection and repeated high strain detection, this paper explores the time-dependent increments in tip resistance, side resistance and total resistance, and believes that the bearing capacity of monopiles cannot be accurately predicted by soil shear and compression parameters, and the axial force increment of monopiles is closely related to depth, which can be accurately predicted by formulas. The main conclusions are as follows:

(1) The total resistance of offshore large diameter monopiles increases by 65%-162% after the 10d-84d rest period.
(2) A method for predicting the time-dependent increment of bearing capacity of offshore large-diameter monopiles is proposed;
(3) In this paper, the prediction is only based on 7.2m-7.4m large diameter monopiles, and the time-dependent of another diameter monopiles still needs to be further verified.

REFERENCES

[1] Xiaoni Wu, Yu Hu, Ye Li, et al. Foundations of offshore wind turbines: A review, Renewable and Sustainable Energy Reviews, 2019, 104: 379-393
[2] Subhamoy Bhattacharya. Design of Foundations for Offshore Wind Turbines, 1st ed.; John Wiley & Sons Ltd.: Chichester, UK, 2019.
[3] Jit Kheng Lim, Barry Lehane. Time effects on shaft capacity of jacked piles in sand, Canadian Geotechnical Journal, 2015, 52: 1830-1838. https://doi.org/10.1139/cgj-2014-0463
[4] Suchun Yang, Junwei Liu, Ankit Garg, et al. Analytical solution for estimating bearing capacity of a closed soil plug: Verification using an On-Site static pile test, Journal of Marine Science and Engineering, 2020, 8: 490. https://doi.org/10.3390/jmse8070490
[5] Suchun Yang, Junwei Liu, Longfei Xu, et al. A new approach to explore the surface profile of clay soil using white light interferometry, Sensors, 2020, 20: 3009. https://doi.org/10.3390/s20113009

[6] Suchun Yang, Junwei Liu, Mingyi Zhang, et al. Analytical solution and field test of critical bearing capacity and settlement of pile tip, CIVIL ENGINEERING JOURNAL-STAVEBNI OBZOR, 2020, 1: 61-74. https://doi.org/10.14311/CEJ.2020.01.0006
[7] Suchun Yang, Mingyi Zhang, Songkui Sang. Dem study on the penetration of jacked piles into layered soft clay, CIVIL ENGINEERING JOURNAL-STAVEBNI OBZOR, 2020, 3: 370-384. https://doi.org/10.14311/CEJ.2020.03.0033
[8] Yang Su-Chun, Zhang Ming-Yi, Wang Yong-Hong, et al. Field test on pile tip resistance of closed-end jacked pipe pile penetrating into layered foundation, ROCK AND SOIL MECHANICS, 2018, 39: 91-99. https://doi.org/10.16285/j.rsm.2018.0961
[9] American Petroleum Institute. Planning, designing, and constructing fixed offshore platforms: working stress design. American Petroleum Institute; 2014.
[10] G. L. DNV. Design of offshore wind turbine structures, DNV GL: Oslo, Norway, 2014.
[11] Matlock H. Correlations for design of laterally loaded piles in soft clay. Proceedings of the 2nd Annual Offshore Technology Conference. Houston: Texas, 1970.
[12] Lymon C. Reese, Robert C. Welch. Lateral loading of deep foundations in stiff clay, Journal of the Geotechnical engineering division, 1975, 101: 633-649
[13] Bin Zhu, Zhou-Jie Zhu, Tao Li, et al. Field tests of offshore driven piles subjected to lateral monotonic and cyclic loads in soft clay, Journal of Waterway Port Coastal and Ocean Engineering, 2017, 143. https://doi.org/10.1061/(ASCE)WW.1943-5460.0000399
[14] Huxinghao, Wang Xing, Lou Xueqian, et al. experimental study on timeliness of large diameter steel pipe piles under complex geological conditions at sea, ocean engineering, 2019, 37: 93-100.
[15] Lin Li, Jingpei Li, De An Sun, et al. Analysis of time-dependent bearing capacity of a driven pile in clayey soils by total stress method, International Journal of Geomechanics, 2017, 17: 4016156.